

# 4 Multiplets in Transition Metal Ions and Introduction to Multiband Hubbard Models

Robert Eder

Institute for Quantum Materials and Technologies

Karlsruhe Institute of Technology

## Contents

<b>1</b>	<b>Introduction</b>	<b>2</b>
<b>2</b>	<b>Multiplets of a free ion</b>	<b>2</b>
2.1	General considerations . . . . .	2
2.2	Matrix elements of the Coulomb interaction . . . . .	5
2.3	Diagonal matrix elements . . . . .	7
2.4	Analytical calculation of multiplet energies by the diagonal sum-rule . . . . .	9
2.5	Solution of the Coulomb problem by exact diagonalization . . . . .	11
2.6	Spin-orbit coupling . . . . .	13
<b>3</b>	<b>Effects of the environment in the crystal</b>	<b>14</b>
3.1	Crystalline electric field . . . . .	14
3.2	Charge transfer . . . . .	19
<b>4</b>	<b>Multiband Hubbard models</b>	<b>23</b>
<b>5</b>	<b>Conclusion</b>	<b>25</b>
<b>A</b>	<b>Gaunt coefficients</b>	<b>26</b>

# 1 Introduction

Compounds containing  $3d$  or  $4f$  transition-metal or rare-earth ions have been intriguing solid state physicists ever since the appearance of solid state physics as a field of research. In fact, already in the 1930's NiO became the first known example of a correlated insulator in that it was cited by deBoer and Verwey as a counterexample to the then newly invented Bloch theory of electron bands in solids [1]. During the last 25 years  $3d$  and  $4f$  compounds have become one of the central fields of solid state physics following the discovery of heavy fermion compounds, cuprate superconductors, the colossal magnetoresistance phenomenon in the manganites and, most recently, the iron-pnictide superconductors.

It was conjectured early on that the reason for the special behavior of these compounds is the strong Coulomb interaction between electrons in their partially filled  $3d$  or  $4f$  shells. The  $3d$  wave functions are orthogonal to those of the inner-shells, such as  $1s$ ,  $2s$ ,  $2p$ ,  $3s$  and  $3p$ , solely due to their angular part  $Y_{2,m}(\vartheta, \varphi)$ . Their radial part  $R_{3,2}(r)$  therefore is not pushed out to regions far from the nucleus by the requirement to be orthogonal to the inner shell wave functions and therefore is concentrated close to the nucleus (the situation is exactly the same for the  $4f$  wave functions). Any two electrons in the  $3d$  shell thus are forced to be close to each other on average so that their mutual Coulomb repulsion is strong (the Coulomb repulsion between two  $3d$  electrons is small, however, when compared to the Coulomb force due to the nucleus and the inner shells so that the electrons *have to* stay close to one another!). For clarity let us mention that the Coulomb repulsion between electrons in the inner shells of heavier elements is actually much stronger than that in the  $3d$  shell of transition metals or the  $4f$  shell of rare earths. This, however, is irrelevant because these inner shells are several 100–1000 eV below the Fermi energy so that they are simply completely filled and inert. On the other hand, the  $3d$  orbitals in transition metal compounds and the  $4f$  orbitals in rare earth compounds participate in the bands at the Fermi level so that the strong Coulomb interaction in these orbitals directly influences the conduction electrons. The conduction bands in such compounds therefore form dense many-body-systems of strongly interacting electrons, where the average energy of interaction is large compared to the average kinetic energy. This dominance of the interaction energy implies a propensity to show ordering phenomena and the ensuing quantum phase transitions and superconducting domes. It is therefore ultimately the Coulomb repulsion in the partially filled  $3d$  shells of the transition metals and the  $4f$  shells of the rare earths which gives rise to the wide variety of spectacular phenomena observed in compounds containing these elements. Let us therefore discuss this Coulomb interaction in more detail.

## 2 Multiplets of a free ion

### 2.1 General considerations

In the following we restrict ourselves to  $3d$  transition metal ions for definiteness, but the theory is easily adapted to other atomic shells. We consider a  $\text{Ni}^{2+}$  ion in vacuum which has the

Term	$J$	E (eV)
${}^3F$	4	0.000
	3	0.169
	2	0.281
${}^1D$	2	1.740
${}^3P$	2	2.066
	1	2.105
	0	2.137
${}^1G$	4	2.865
${}^1S$	0	6.514

**Table 1:** Energies of the multiplets of  $Ni^{2+}$  from Ref. [2].  $J$  is the total angular momentum quantum number and the  $J = 4$  member of  ${}^3F$  has been taken as the zero of energy.

electron configuration  $[Ar] 3d^8$ . It is a standard exercise in textbooks of atomic physics to show that the  $d^8$  configuration has the following multiplets or terms:  ${}^3F$ ,  ${}^3P$ ,  ${}^1G$ ,  ${}^1D$  and  ${}^1S$ , whereby according to the first two Hund's rules  ${}^3F$  is the ground state. 'Multiplets' thereby is simply another word for 'eigenstates of 8 electrons in the electric field of the Ni nucleus and the Ar core' (the electrons in the shells below  $3d$  may be considered as inert due to the large binding energies of these shells). The energies of the multiplets can be deduced experimentally for example by analyzing the optical spectrum of Ni vapor and are listed in Table 1. They span a range of several eV whereby multiplets with nonzero spin are in addition split by spin-orbit coupling which results in intervals of order 0.1 eV. All of these eigenstates correspond to the same electron configuration, namely  $[Ar] 3d^8$ , so that the fact that, say,  ${}^3P$  has a higher energy than  ${}^3F$  is not due to an electron having been promoted from a state with low energy to one with high energy as in an optical transition. Rather, the excited multiplets —  ${}^3P$ ,  ${}^1G$ ,  ${}^1D$  and  ${}^1S$  — should be viewed as *collective excitations* of the 8-electron system, similar in nature to a plasmon in an electron gas. And just as a plasmon can exist only due to the Coulomb interaction between electrons, the multiplet splitting in atomic shells also originates from the Coulomb interaction between electrons. This is what we discuss next.

As a first step we introduce Fermionic creation and annihilation operators  $c_{n,l,m,\sigma}^\dagger$  which create an electron with  $z$ -component of spin  $\sigma$  in the orbital with principal quantum number  $n$ , orbital angular momentum  $l$ , and  $z$ -component of orbital angular momentum  $m$ . In the case of a partly filled  $3d$  shell all  $n_i = 3$  and all  $l_i = 2$  identically, so that these two indices could be omitted, but we will keep them for the sake of generality. In the following we will often contract  $(n, l, m, \sigma)$  to the 'compound index'  $\nu$  for brevity, so that, e.g.,  $c_{\nu_i}^\dagger = c_{n_i, l_i, m_i, \sigma_i}^\dagger$ .

The procedure we follow is degenerate first-order perturbation theory as discussed in practically any textbook of quantum mechanics. The unperturbed Hamiltonian  $H_0$  thereby corresponds to the energies of the different atomic shells

$$H_0 = \sum_{n,l} \varepsilon_{n,l} \sum_{m,\sigma} c_{n,l,m,\sigma}^\dagger c_{n,l,m,\sigma}$$

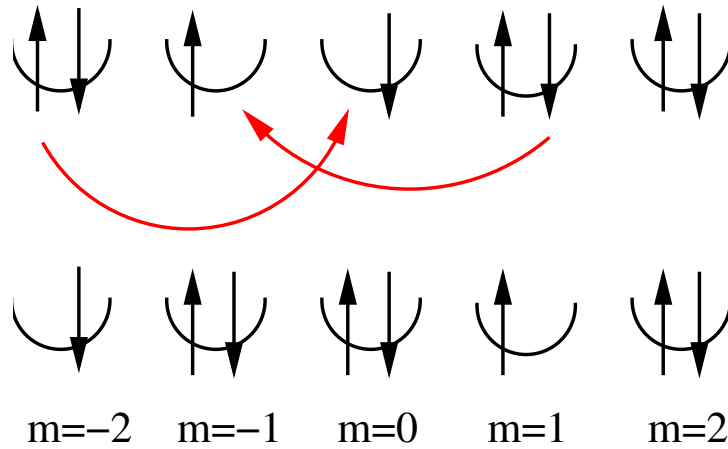


**Fig. 1:** Coulomb scattering of two electrons in the  $d$ -shell. In the initial state  $|\nu\rangle$  (top) the electrons are distributed over the five  $d$ -orbitals which are labeled by their  $m$ -values. Due to their Coulomb interaction two electrons scatter from each other and are simultaneously transferred to different orbitals, resulting in the state  $|\mu\rangle$  (bottom).

whereas the Coulomb interaction is considered as the perturbation  $H_1$  (we ignore spin-orbit coupling for the time being). The  $d^n$  configuration comprises all states which are obtained by distributing  $n$  electrons over the  $2 \cdot 5 = 10$  spin-orbitals:

$$|\nu\rangle = |\nu_1, \nu_2 \dots \nu_n\rangle = c_{\nu_1}^\dagger c_{\nu_2}^\dagger \dots c_{\nu_n}^\dagger |0\rangle, \quad (1)$$

and the number of these states obviously is  $n_c = 10!/(n!(10-n)!)$ . In writing the basis states as in (1) we need to specify an ordering convention for the creation operators on the right hand side. For example, only states are taken into account where  $m_1 \leq m_2 \leq m_3 \dots \leq m_n$ . Moreover, if two  $m_i$  are equal the  $c_{m_i, \downarrow}^\dagger$ -operator is assumed to be to the left of the  $c_{m_i, \uparrow}^\dagger$ -operator. If we adopt this convention, every possible state obtained by distributing the  $n$  electrons over the 10 spin-orbitals is included exactly once in the basis. If the  $n_i$  and  $l_i$  were to take different values we could generalize this, e.g., by demanding that the  $(n_i, l_i, m_i)$ -triples be ordered lexicographically. As will be seen later, strict application of an ordering convention for the Fermi operators is necessary to determine the correct Fermi signs for the matrix elements.

If only  $H_0$  were present all states (1) would be degenerate with energy  $E = E[Ar] + n \cdot \varepsilon_{3,2}$ , where  $E[Ar]$  is the energy of the Argon core. The Coulomb interaction  $H_1$  between the electrons (partially) lifts this degeneracy and this is the physical reason for the multiplet splitting. The standard procedure in degenerate first order perturbation theory is to set up the secular matrix  $h_{\mu, \nu} = \langle \mu | H_1 | \nu \rangle$  and diagonalize it to obtain the first order energies and wave functions [3]. The diagonal matrix elements  $\langle \nu | H_1 | \nu \rangle$  describe the fact that the Coulomb repulsion between two electrons in different orbitals depends on the spatial character of these orbitals, whereas the off-diagonal matrix elements  $\langle \mu | H_1 | \nu \rangle$  describe the scattering of two electrons ‘within the  $3d$  shell’ as shown in Figure 1.

In second quantization the Coulomb Hamiltonian  $H_1$  takes the form

$$H_1 = \frac{1}{2} \sum_{\nu_1, \nu_2, \nu_3, \nu_4} V(\nu_1, \nu_2, \nu_3, \nu_4) c_{\nu_1}^\dagger c_{\nu_2}^\dagger c_{\nu_3} c_{\nu_4},$$

$$V(\nu_1, \nu_2, \nu_3, \nu_4) = \int dx \int dx' \psi_{\nu_1}^*(x) \psi_{\nu_2}^*(x') V_c(x, x') \psi_{\nu_4}(x) \psi_{\nu_3}(x'),$$

$$V_c(x, x') = \frac{1}{|\mathbf{r} - \mathbf{r}'|}. \quad (2)$$

Here  $x = (\mathbf{r}, \sigma)$  is the combined position and spin coordinate with  $\int dx \cdots = \sum_\sigma \int d\mathbf{r} \cdots$  and  $V_c$  is the Coulomb interaction between electrons. Note the factor of  $1/2$  in front of  $H_1$  and the correspondence of indices and integration variables  $\nu_4 \leftrightarrow x$  and  $\nu_3 \leftrightarrow x'$  in the Coulomb matrix element, see textbooks of many-particle physics such as Fetter-Walecka [6].

## 2.2 Matrix elements of the Coulomb interaction

Our single-particle basis consists of atomic spin-orbitals so if we switch to spherical coordinates  $(r, \vartheta, \varphi)$  for  $\mathbf{r}$  the wave functions in (2) are

$$\psi_{\nu_i}(x) = R_{n_i, l_i}(r) Y_{l_i, m_i}(\vartheta, \varphi) \delta_{\sigma, \sigma_i}. \quad (3)$$

For a table of spherical harmonics  $Y_{l, m}$  see Ref. [4]. The radial wave functions  $R_{n_i, l_i}$  are assumed to be real — as is the case for the true radial wave function of bound states in a central potential. Apart from that we do not really specify them. It will turn out that these radial wave functions enter the Coulomb matrix elements only via a discrete and rather limited set of real numbers which are often obtained by a fit to experiment.

In addition to (3), we use the familiar multipole expansion of the Coulomb interaction [5]

$$\frac{1}{|\mathbf{r} - \mathbf{r}'|} = \sum_{k=0}^{\infty} \sum_{m=-k}^k Y_{k, m}^*(\vartheta', \varphi') \frac{4\pi}{2k+1} \frac{r_{<}^k}{r_{>}^{k+1}} Y_{k, m}(\vartheta, \varphi). \quad (4)$$

We now insert (3) and (4) into (2). We recall that  $\int dx \cdots = \sum_\sigma \int d\mathbf{r} \cdots$  and first carry out the sums over spin variables:

$$\sum_{\sigma, \sigma'} \delta_{\sigma, \sigma_1} \delta_{\sigma', \sigma_2} \delta_{\sigma, \sigma_4} \delta_{\sigma', \sigma_3} = \delta_{\sigma_1, \sigma_4} \delta_{\sigma_2, \sigma_3}.$$

This reflects the fact that since the Coulomb interaction does not depend on spin, the spins of the two electrons are conserved in the Coulomb scattering. Next, we pick one term with given  $k$  and  $m$  from the multipole expansion (4) and proceed to the integration over the spatial variables  $(r, \vartheta, \varphi)$  and  $(r', \vartheta', \varphi')$ . Let us first consider  $(\vartheta, \varphi)$  and adopt the compact notation  $(\vartheta, \varphi) = \Omega$ . These variables always come as arguments of spherical harmonics and there is one from  $\psi_{\nu_1}^*(x)$ , one from the multipole expansion (4), and one from  $\psi_{\nu_4}(x)$ . We obtain the integral

$$\int d\Omega Y_{l_1, m_1}^*(\Omega) Y_{k, m}(\Omega) Y_{l_4, m_4}(\Omega), \quad (5)$$

where  $\int d\Omega \cdots = \int_0^{2\pi} d\varphi \int_{-1}^1 d\cos(\vartheta) \dots$ . Such a dimensionless integral over three spherical harmonics is called a Gaunt coefficient and it follows from the Wigner-Eckart theorem that it is proportional to a Clebsch-Gordan coefficient [7, 8].

Next we recall  $Y_{l,m}(\vartheta, \varphi) = P_{l,m}(\vartheta) e^{im\varphi}$  [3] whence the integral (5) is proportional to

$$\int_0^{2\pi} d\varphi e^{-i(m_1-m-m_4)\varphi} = \delta_{m,m_1-m_4}.$$

We introduce the following notation for nonvanishing Gaunt coefficients

$$c^k(lm; l'm') = \sqrt{\frac{4\pi}{2k+1}} \int d\Omega Y_{l,m}^*(\Omega) Y_{k,m-m'}(\Omega) Y_{l',m'}(\Omega),$$

where we have also included ‘half of the factor  $\frac{4\pi}{2k+1}$ ’ from (4). Then, (5) becomes

$$\sqrt{\frac{4\pi}{2k+1}} \int d\Omega Y_{l_1,m_1}^*(\Omega) Y_{k,m}(\Omega) Y_{l_4,m_4}(\Omega) = \delta_{m,m_1-m_4} c^k(l_1m_1; l_4m_4). \quad (6)$$

Since the remaining  $\vartheta$ -dependent factors  $P_{l,m}(\vartheta)$  are real [3] it follows that all Gaunt coefficients are real as well. Using this property the integral over  $(\vartheta', \varphi')$  becomes

$$\sqrt{\frac{4\pi}{2k+1}} \int d\Omega' Y_{l_2,m_2}^*(\Omega') Y_{k,m}^*(\Omega') Y_{l_3,m_3}(\Omega') = \delta_{m,m_3-m_2} c^k(l_3m_3; l_2m_2). \quad (7)$$

Since both (6) and (7) must be different from zero for the *same*  $m$  in order to obtain a nonvanishing contribution, we must have  $m_1-m_4 = m_3-m_2$  or  $m_1+m_2 = m_3+m_4$ , i.e., the total  $L^z$  is conserved in the scattering process. This could have been expected from the very beginning and our formalism incorporates this.

It remains to do the integral over the two radial variables  $r$  and  $r'$ . These two integrations cannot be disentangled so we find a factor of

$$R^k(n_1l_1, n_2l_2, n_3l_3, n_4l_4) = \int_0^\infty dr r^2 \int_0^\infty dr' r'^2 R_{n_1,l_1}(r) R_{n_2,l_2}(r') \frac{r^k}{r^{k+1}} R_{n_4,l_4}(r) R_{n_3,l_3}(r'). \quad (8)$$

These integrals have the same dimension as  $V_c$ , i.e., energy. Collecting everything we find

$$V(\nu_1, \nu_2, \nu_3, \nu_4) = \sum_{k=0}^{\infty} c^k(l_1m_1; l_4m_4) c^k(l_3m_3; l_2m_2) R^k(n_1l_1, n_2l_2, n_3l_3, n_4l_4) \quad (9)$$

$$\times \delta_{\sigma_1,\sigma_4} \delta_{\sigma_2,\sigma_3} \delta_{m_1+m_2,m_3+m_4}.$$

The number of relevant multipole orders  $k$  in this sum is severely limited by the properties of the Gaunt coefficients  $c^k(lm; l'm')$ . First, since these are proportional to Clebsch-Gordan coefficients the three  $l$ -values appearing in them have to obey the so-called *triangular condition* [3]  $k \leq \min(l, l')$  whence  $k \leq \min(l_1+l_4, l_2+l_3)$ . For Coulomb scattering in a  $d$  shell all  $l_i = 2$  whence  $k \leq 4$ . Second, the parity of the spherical harmonic  $Y_{lm}$  is  $(-1)^l$ . For Coulomb scattering within a given atomic shell all  $l_i$  are equal and for integrals such as (5) or (7) to be different from zero the spherical harmonic  $Y_{k,m}$  from the multipole expansion must have

positive parity whence  $k$  must be even. For Coulomb scattering within a  $d$  shell therefore only  $R^0$ ,  $R^2$  and  $R^4$  are relevant. This shows that the sloppy definition of the radial wave function  $R_{n_i, l_i}(r)$  is not a real problem because details of this wave function are irrelevant anyway. In a way, these three parameters may be viewed as a generalization of the Hubbard- $U$  in that  $R^k$  is something like the ‘the Hubbard- $U$  for  $k$ -pole interaction’. Lastly we note that the  $c^k(lm; l'm')$  are tabulated in Appendix 20a of the textbook by Slater [7] or Table 4.4 of the textbook by Griffith [8], and also in the Appendices I and II of the present note.

### 2.3 Diagonal matrix elements

The expression (9) is exact but somewhat complicated so let us try to elucidate its physical content and thereby also make contact with various approximate ways to describe the Coulomb interaction which can be found in the literature. We recall

$$H_1 = \frac{1}{2} \sum_{\nu_1, \nu_2, \nu_3, \nu_4} V(\nu_1, \nu_2, \nu_3, \nu_4) c_{\nu_1}^\dagger c_{\nu_2}^\dagger c_{\nu_3} c_{\nu_4},$$

and pick those terms from  $H_1$  where either  $\nu_4 = \nu_1$  and  $\nu_3 = \nu_2$  (case 1) or  $\nu_3 = \nu_1$  and  $\nu_4 = \nu_2$  (case 2). Notice that the Pauli principle requires  $\nu_1 \neq \nu_2$  — otherwise  $H_1$  contains the product  $c_{\nu_1}^\dagger c_{\nu_1}^\dagger = 0$ . In both cases the four Fermion operators can be permuted to give the product of number operators  $n_{\nu_1} n_{\nu_2}$  (with  $n_\nu = c_\nu^\dagger c_\nu$ ) whereby in case 2 an odd number of interchanges of Fermion operators is necessary so that an additional factor of  $(-1)$  appears. Since  $\nu_1 \neq \nu_2$  no nonvanishing anticommutators arise in this permutation of operators. Whereas for case 1 the product  $\delta_{\sigma_1, \sigma_4} \delta_{\sigma_2, \sigma_3}$  in (9) always is 1, it vanishes for case 2 unless  $\sigma_1 = \sigma_2$ . We had  $\nu_1 \neq \nu_2$  so that for case 1 the two orbitals may have the same orbital quantum numbers  $n, l, m$  but then must differ in their spin, whereas in case 2 the spins have to be equal so that the orbital quantum numbers definitely must be different. Using (9) the respective matrix elements are

$$\begin{aligned} V(\nu_1, \nu_2, \nu_2, \nu_1) &= \sum_{k=0}^{\infty} c^k(l_1 m_1; l_1, m_1) c^k(l_2 m_2; l_2, m_2) R^k(n_1 l_1, n_2 l_2, n_2 l_2, n_1 l_1), \\ V(\nu_1, \nu_2, \nu_1, \nu_2) &= \delta_{\sigma_1, \sigma_2} \sum_{k=0}^{\infty} c^k(l_1 m_1; l_2, m_2) c^k(l_1 m_1; l_2, m_2) R^k(n_1 l_1, n_2 l_2, n_1 l_1, n_2 l_2). \end{aligned} \quad (10)$$

It is customary to introduce the abbreviations

$$\begin{aligned} a^k(lm; l'm') &= c^k(lm; lm) c^k(l'm'; l'm') \\ b^k(lm; l'm') &= c^k(lm; l'm') c^k(lm; l'm') \\ F^k(nl; n'l') &= R^k(nl, n'l', n'l', nl) \\ G^k(nl; n'l') &= R^k(nl, n'l', nl, n'l') \end{aligned} \quad (11)$$

The  $F^k$  and  $G^k$  are called Slater-Condon parameters. The  $a^k$  and  $b^k$  are listed in Appendix 20a of Slater’s textbook [7] and also in the Appendix of the present note.

We want to bring these diagonal matrix elements to a more familiar form and continue to specialize to a partly filled  $3d$  shell. In this case all  $n_i = 3$  and  $l_i = 2$  so that for each  $k$  there

is only one  $F^k$  and one  $G^k$  and, in fact,  $G^k = F^k$ . For brevity we omit the  $n$ - and  $l$  quantum numbers in the rest of the paragraph so that, e.g., the electron operators become  $c_{m,\sigma}^\dagger$  where  $m$  is the  $z$ -component of  $\mathbf{L}$ . The sum of all diagonal matrix elements then becomes

$$H_{1,diag} = \sum_m U_{m,m} n_{m,\uparrow} n_{m,\downarrow} + \frac{1}{2} \sum_{m \neq m'} \left( U_{m,m'} \sum_{\sigma,\sigma'} n_{m,\sigma} n_{m',\sigma'} - J_{m,m'} \sum_{\sigma} n_{m,\sigma} n_{m',\sigma} \right),$$

$$U_{m,m'} = \sum_{k \in \{0,2,4\}} a^k(m, m') F^k, \quad J_{m,m'} = \sum_{k \in \{0,2,4\}} b^k(m, m') F^k. \quad (12)$$

The first term on the r.h.s. originates from case 1 with  $m_1 = m_2$  and the factor of  $\frac{1}{2}$  in front of this term is cancelled because there are two identical terms of this type with either  $\nu_1 = (m, \uparrow)$  and  $\nu_2 = (m, \downarrow)$  or  $\nu_1 = (m, \downarrow)$  and  $\nu_2 = (m, \uparrow)$ . We introduce the operators of electron density  $n_m = n_{m,\uparrow} + n_{m,\downarrow}$  and electron spin  $S_m^z = \frac{1}{2}(n_{m,\uparrow} - n_{m,\downarrow})$  and rewrite

$$\sum_{\sigma,\sigma'} n_{m,\sigma} n_{m',\sigma'} = n_m n_{m'} \quad \sum_{\sigma} n_{m,\sigma} n_{m',\sigma} = 2 \left( S_m^z S_{m'}^z + \frac{n_m n_{m'}}{4} \right),$$

so that

$$H_{1,diag} = \sum_m U_{m,m} n_{m,\uparrow} n_{m,\downarrow} + \frac{1}{2} \sum_{m \neq m'} \left( (U_{m,m'} - \frac{1}{2} J_{m,m'}) n_m n_{m'} - 2 J_{m,m'} S_m^z S_{m'}^z \right). \quad (13)$$

This is the sum of a density-density interaction  $\propto U_{m,m'}$  and an Ising-like spin interaction  $\propto J_{m,m'}$ . The interaction parameters depend on the orbitals and can be expressed in terms of the Slater-Condon parameters  $F^k$  and the products of Gaunt coefficients  $a^k$  and  $b^k$ . It is obvious from (11) and (12) that  $J_{m,m'} > 0$  so that the spin interaction is ferromagnetic — this is in fact the physical origin of the first Hund's rule.

To complete the Hund's rule term we pick those terms in  $H_1$  where  $\nu_1 = (m, \sigma)$ ,  $\nu_2 = (m', \bar{\sigma})$ ,  $\nu_3 = (m, \bar{\sigma})$  and  $\nu_4 = (m', \sigma)$ . In these terms the product  $\delta_{\sigma_1, \sigma_4} \delta_{\sigma_2, \sigma_3}$  is non-vanishing as well and for both values of  $\sigma$  the matrix element (2) is

$$\sum_{k \in \{0,2,4\}} c^k(m, m') c^k(m, m') F^k = \sum_{k \in \{0,2,4\}} b^k(m, m') F^k = J_{m,m'}$$

The Fermion operators are  $c_{m,\uparrow}^\dagger c_{m',\downarrow}^\dagger c_{m,\downarrow} c_{m',\uparrow} + c_{m,\downarrow}^\dagger c_{m',\uparrow}^\dagger c_{m,\uparrow} c_{m',\downarrow} = -(S_m^+ S_{m'}^- + S_m^- S_{m'}^+)$ , i.e., the transverse part of the Heisenberg exchange. Combining these terms with the Ising-like spin exchange term we obtain

$$H_{1,H} = \sum_m U_{m,m} n_{m,\uparrow} n_{m,\downarrow} + \frac{1}{2} \sum_{m \neq m'} \left( (U_{m,m'} - \frac{1}{2} J_{m,m'}) n_m n_{m'} - 2 J_{m,m'} \mathbf{S}_m \cdot \mathbf{S}_{m'} \right). \quad (14)$$

This is now the sum of a density-density interaction and a spin-rotation invariant ferromagnetic spin exchange. It has to be kept in mind that this Hamiltonian has been obtained by retaining only a relatively small subset of matrix elements in the original Coulomb Hamiltonian. A



further simplification which is often used is to replace  $U_{m,m'}$  and  $J_{m,m'}$  by their averages over all corresponding pairs  $(m, m')$ . Using the  $a^k$  and  $b^k$  in the Appendix one readily obtains

$$U = \frac{1}{25} \sum_{m,m'} U_{m,m'} = F^0,$$

$$U - J = \frac{1}{20} \sum_{m \neq m'} (U_{m,m'} - J_{m,m'}) = F^0 - \frac{1}{14} (F^2 + F^4),$$

so that  $J = (F^2 + F^4)/14$ .

To conclude the discussion we consider the diagonal matrix elements  $\langle \nu | H_1 | \nu \rangle$  in the basis of  $n$ -electron states  $|\nu\rangle$  defined in (1). Since  $\nu_1$  and  $\nu_2$  in (10) can be any two out of the  $n$  occupied orbitals in  $|\nu\rangle$  the total diagonal matrix element of  $H_1$  is obtained by summing over all  $n(n-1)/2$  pairs  $(i, j)$  formed from the occupied orbitals

$$\langle \nu | H_1 | \nu \rangle = \sum_{i < j} \sum_k \left( a^k(l_i m_i, l_j, m_j) F^k(n_i l_i, n_j l_j) - \delta_{\sigma_i \sigma_j} b^k(l_i m_i, l_j, m_j) G^k(n_i l_i, n_j l_j) \right). \quad (15)$$

As will be seen in the next paragraph, this formula is actually sufficient to calculate the multiplet energies.

## 2.4 Analytical calculation of multiplet energies by the diagonal sum-rule

We now show that the theory developed so far is in fact sufficient to give analytical formulas for the energies of the multiplets which can be compared to experiment. The first ingredient is the so-called diagonal sum-rule. This is simply the well-known theorem that the sum of the eigenvalues of a Hermitean matrix  $H$  is equal to its trace  $\text{tr}(H) = \sum_i H_{ii}$ . It follows immediately by noting that the trace of a matrix is invariant under basis transformations, i.e.,  $\text{tr}(H) = \text{tr}(U H U^{-1})$  for any unitary matrix  $U$ . By choosing  $U$  to be the matrix which transforms to the basis of eigenvectors of  $H$  the diagonal sum-rule follows immediately.

Next, one uses the fact that the Hamilton matrix is block-diagonal, with blocks defined by their values of  $L^z$  and  $S^z$  — this is the consequence of the  $\delta$ -functions in (9). The diagonal sum-rule then can be applied separately for each of these blocks. In addition, the dimension of the blocks decreases as  $L^z$  and  $S^z$  approach their maximum possible values so that the number of multiplets contained in a given block decreases and the multiplet energies are easy to read off.

As an example for the procedure let us consider a  $p^2$  configuration (by particle-hole symmetry this is equivalent to a  $p^4$  configuration). We write the Fermion operators in the form  $c_{l,m,\sigma}^\dagger$ , i.e., we suppress the principal quantum number  $n$ . Since we have 6 possible states for a single  $p$ -electron - three  $m$ -values and two spin directions per  $m$ -value — we have 15 states for two electrons. The triangular condition for the Gaunt coefficients now restricts the multipole order  $k$  to be  $\leq 2$ . Again, only even  $k$  contribute, so that we have two Slater-Condon parameters,  $F^0$  and  $F^2$  (and  $G^k = F^k$ ). Table 2, which is taken from Slater's textbook [7], gives the values of the coefficients  $a^k(1, m; 1, m')$  and  $b^k(1, m; 1, m')$ .

$m$	$m'$	$a^0$	$25a^2$	$b^0$	$25b^2$
$\pm 1$	$\pm 1$	1	1	1	1
$\pm 1$	0	1	-2	0	3
0	0	1	4	1	4
$\pm 1$	$\mp 1$	1	1	0	6

**Table 2:** The coefficients  $a^k$  and  $b^k$  for two  $p$ -electrons.

We first consider the sector with  $S^z = 1$ . The highest possible  $L^z$  is  $L^z = 1$  which is realized only for a single state,  $|1\rangle = c_{1,0,\uparrow}^\dagger c_{1,1,\uparrow}^\dagger |0\rangle$ . We can conclude that one of the multiplets is  ${}^3P$  and its energy is equal to the diagonal matrix element of  $|1\rangle$  which by (15) is

$$E({}^3P) = \sum_{k \in \{0,2\}} \left( a^k(1, 1; 1, 0) - b^k(1, 1; 1, 0) \right) F^k = F^0 - \frac{5}{25} F^2.$$

We proceed to the sector  $S^z = 0$ . Here the highest possible  $L^z$  is  $L^z = 2$  again obtained for only single state namely  $c_{1,1,\downarrow}^\dagger c_{1,1,\uparrow}^\dagger |0\rangle$ . We conclude that we also have  ${}^1D$  with energy

$$E({}^1D) = \sum_{k \in \{0,2\}} a^k(1, 1; 1, 1) F^k = F^0 + \frac{1}{25} F^2.$$

The two multiplets that we found so far,  ${}^1D$  and  ${}^3P$ , comprise  $5 + 9 = 14$  states; we thus have just one state missing, which can only be  ${}^1S$ . To find its energy, we need to consider the sector  $S^z = 0$  and  $L^z = 0$ . There are three states in this sector:  $c_{1,0,\downarrow}^\dagger c_{1,0,\uparrow}^\dagger |0\rangle$ ,  $c_{1,-1,\uparrow}^\dagger c_{1,1,\downarrow}^\dagger |0\rangle$  and  $c_{1,-1,\downarrow}^\dagger c_{1,1,\uparrow}^\dagger |0\rangle$ . Two out of the three eigenvalues of the  $3 \times 3$  Hamiltonian in the basis spanned by these states must be  $E({}^3P)$  and  $E({}^1D)$ , because these multiplets also have members with  $S^z = 0$  and  $L^z = 0$ . To obtain  $E({}^1S)$  we accordingly compute the sum of the diagonal elements of the  $3 \times 3$  matrix using (15) and set

$$\begin{aligned} E({}^3P) + E({}^1D) + E({}^1S) &= \sum_{k \in \{0,2\}} \left( a^k(1, 0; 1, 0) + 2 a^k(1, -1; 1, 1) \right) F^k, \\ \rightarrow E({}^1S) &= F^0 + \frac{10}{25} F^2. \end{aligned}$$

This example shows the way of approach for multiplet calculations using the diagonal sum-rule: one starts out with a state with maximum  $L^z$  or  $S^z$  for which there is usually only a single basis state. This basis state belongs to some multiplet whose energy simply equals the ‘diagonal element’ of the  $1 \times 1$  Hamiltonian. Then one proceeds to lower  $S^z$  and/or  $L^z$  and obtains energies of additional multiplets by calculating the trace of the respective block of the Hamilton matrix and using the known energies of multiplets with higher  $L^z$  or  $S^z$ . It turns out that in this way the energies of *all* multiplets involving  $s$ ,  $p$ ,  $d$  or  $f$  electrons can be expressed in terms of the Slater-Condon parameters by analytical formulas. A rather complete list can be found for example in the Appendices 21a and 21 of the textbook by Slater [7].

Multiplet theory was originally developed to discuss the spectra of atoms or ions in the gas phase. The question then arises, as to what are the values of the Slater-Condon parameters.

	Si	P <sup>+</sup>	S <sup>2+</sup>	S	Cl <sup>+</sup>
<sup>3</sup> P	0.0000	0.0000	0.0000	0.0000	0.0000
<sup>1</sup> D	0.7809	1.1013	1.4038	1.1454	1.4449
<sup>1</sup> S	1.9087	2.6750	3.3675	2.7500	3.4564
r	1.4442	1.4289	1.3988	1.4010	1.3921

**Table 3:** Energies (in eV) of multiplets for different atoms and ions with  $p^2$  or  $p^4$  configurations outside a closed shell (taken from the NIST data base [2]) and the resulting values of  $r$  in (16).

Of course one might attempt to compute these parameters using, e.g., Hartree-Fock wave functions in the expression (8). It turns out, however, that very frequently the number of multiplets considerably exceeds the number of relevant Slater-Condon parameters. In the case of the  $p^2$  configuration we had three multiplets,  $^3P$ ,  $^1D$  and  $^1S$ , but only two Slater-Condon parameters  $F^0$  and  $F^2$ . This would suggest to obtain the values of the Slater-Condon parameters by fit to the spectroscopic data and the textbook by Slater [7] contains a vast amount of experimental data which are analyzed in this way. For the  $p^2$  configuration we restrict ourselves to a simple cross check. Using the above expressions we find

$$r = \frac{E(^1S) - E(^1D)}{E(^1D) - E(^3P)} = \frac{3}{2}, \quad (16)$$

*independently* of the values of  $F^0$  and  $F^2$ . This relation therefore should be obeyed by all ions with two  $p$ -electrons outside filled shells, such as the series Si, P<sup>1+</sup>, S<sup>2+</sup>, or two holes in a filled  $p$ -shell such as the series S, Cl<sup>+</sup>. The energies of the multiplets of these atoms/ions are available in the database [2] and Table 3 shows the energies and the resulting values of  $r$ .

They are in fact quite close  $3/2$ . Notice that the width of the multiplet spectrum increases considerable when going to the positively charge ions. This is because in positively charged ions the radial wave functions are more contracted, whence the values of the Slater-Condon parameters increase. Despite this, the ratio  $r$  is quite constant and in good agreement with multiplet theory.

## 2.5 Solution of the Coulomb problem by exact diagonalization

Using the diagonal sum rule one can derive analytical formulae for the energies of the multiplets. For further applications of multiplet theory, however, it is often useful to solve the problem numerically, using the method of exact diagonalization which will be outlined in the following. The basis states (1) correspond to all possible ways of distributing  $n$  electrons over the 10 spin-orbitals of the  $3d$ -shell (two spin directions for each  $m \in \{-2, -1, \dots, 2\}$ ). As illustrated in Figure 2 we can code each of these basis states by an integer  $0 \leq i \leq 2^{10}$ . If we really use all of these integers we are actually treating all states with  $0 \leq n \leq 10$  simultaneously but this will be convenient for generalizations of the theory. Next, for a given initial state  $|\nu_1, \nu_2, \dots, \nu_n\rangle$  we can let the computer search for all possible transitions of the type shown in Figure 2 and compute the corresponding matrix elements from (9) using, say, the  $c^k(lm; l'm')$  copied from

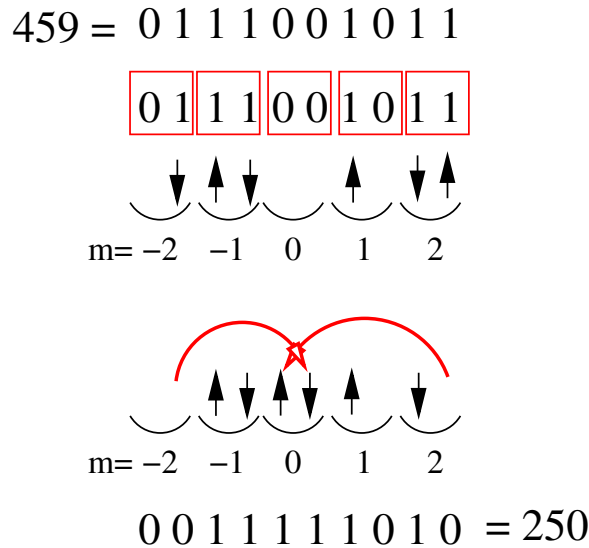


**Fig. 2:** The coding of basis states by integers and a scattering process.

Slater's textbook and some given  $R^0$ ,  $R^2$  and  $R^4$ . Let us consider the following matrix element of a term in  $H_1$  between two states with  $n$  electrons:

$$\langle \mu | V(\lambda_1, \lambda_2, \lambda_3, \lambda_4) c_{\lambda_1}^\dagger c_{\lambda_2}^\dagger c_{\lambda_3} c_{\lambda_4} | \nu \rangle =$$

$$\langle 0 | c_{\mu_n} \dots c_{\mu_1} V(\lambda_1, \lambda_2, \lambda_3, \lambda_4) c_{\lambda_1}^\dagger c_{\lambda_2}^\dagger c_{\lambda_3} c_{\lambda_4} c_{\nu_1}^\dagger c_{\nu_2}^\dagger \dots c_{\nu_n}^\dagger | 0 \rangle.$$

For this to be nonzero, the operators  $c_{\lambda_3}^\dagger$  and  $c_{\lambda_4}^\dagger$  must be amongst the  $c_{\nu_i}^\dagger$ , otherwise the annihilation operators in the Hamiltonian,  $c_{\lambda_3}$  and  $c_{\lambda_4}$ , could be commuted to the right where they annihilate  $|0\rangle$ . In order for  $c_{\lambda_4}$  to 'cancel'  $c_{\lambda_4}^\dagger$  it must first be commuted to the position right in front of  $c_{\lambda_4}^\dagger$ . If this takes  $n_4$  interchanges of Fermion operators we get a Fermi sign of  $(-1)^{n_4}$ . Bringing next  $c_{\lambda_3}$  right in front of  $c_{\lambda_3}^\dagger$  by  $n_3$  interchanges of Fermion operators gives a sign of  $(-1)^{n_3}$ . Analogously,  $c_{\lambda_1}$  and  $c_{\lambda_2}$  must be amongst the  $c_{\mu_i}$  and the creation operators  $c_{\lambda_1}^\dagger$  and  $c_{\lambda_2}^\dagger$  in the Hamiltonian have to be commuted to the left to stand to the immediate right of their respective 'partner annihilation operator' so as to cancel it. If this requires an additional number of Fermion interchanges  $n_1$  for  $c_{\lambda_1}^\dagger$  and  $n_2$  for  $c_{\lambda_2}^\dagger$  there is an additional Fermi sign of  $(-1)^{n_1+n_2}$ . The total matrix element therefore is  $(-1)^{n_1+n_2+n_3+n_4} V(\lambda_1, \lambda_2, \lambda_3, \lambda_4)$ . The correct Fermi sign is crucial for obtaining correct results and must be evaluated by keeping track of all necessary interchanges of Fermion operators. The necessity to determine the Fermi sign is the very reason why we have to adopt an ordering convention and strictly adhere to it.

Once the matrix  $\langle \mu | H_1 | \nu \rangle$  has been set up it can be diagonalized numerically. The following Table 4 gives the resulting multiplet energies for  $d^8$  and  $d^7$ , the values of  $L$  and  $S$  for each multiplet and the degeneracy  $n$ . The values of the  $R^k$  parameters have been calculated [9] by using Hartree-Fock wave functions  $R_{3,2}$  for  $\text{Ni}^{2+}$  and  $\text{Co}^{2+}$  in (8). The energy of the lowest multiplet is taken as the zero of energy and it turns out that all *energy differences* depend only on  $R^2$  and  $R^4$ . Note the increasing complexity of the level schemes with increasing number of holes in the  $d$ -shell. Comparing the energies of the multiplets for  $d^8$  with the experimental values in

E	S	L	n	Term	E	S	L	n	Term
0.0000	1	3	21	${}^3F$	0.0000	3/2	3	28	${}^4F$
1.8420	0	2	5	${}^1D$	1.8000	3/2	1	12	${}^4P$
1.9200	1	1	9	${}^3P$	2.1540	1/2	4	18	${}^2G$
2.7380	0	4	9	${}^1G$	2.7540	1/2	5	22	${}^2H$
13.2440	0	0	1	${}^1S$	2.7540	1/2	1	8	${}^2P$
					3.0545	1/2	2	10	${}^2D$
					4.5540	1/2	3	14	${}^2F$
					9.9774	1/2	2	10	${}^2D$

**Table 4:** Energies of the  $d^8$  multiplets calculated with  $R^2 = 10.479$  eV,  $R^4 = 7.5726$  eV (Left), and energies of the  $d^7$  multiplets calculated with  $R^2 = 9.7860$  eV,  $R^4 = 7.0308$  eV (Right).

Table 1 one can see good agreement with deviations of order 0.1 eV. The only exception is  ${}^1S$ . This is hardly a surprise because here the theoretical energy is  $\approx 13$  eV which is comparable to the difference in energy between the  $3d$  and the  $4s$  shell in Ni (which is  $\approx 10$  eV). It follows that the basic assumption of the calculation, namely that the separation between atomic shells is large compared to the multiplet splitting, is not fulfilled for this special multiplet. To treat  ${}^1S$  more quantitatively it would likely be necessary to include basis states with configurations like  $3d^7 4s^1$ , or, put another way, to consider the screening of the Coulomb interaction by particle-hole excitations from the  $3d$  into the  $4s$  shell.

Finally, the Table shows that the ground states indeed comply with the two first Hund's rules: they have maximum spin and maximum orbital angular momentum for this spin. It can be shown that this is indeed always the case as long as one uses Coulomb and exchange integrals with the correct, i.e. positive, sign [7, 8].

## 2.6 Spin-orbit coupling

So far we have neglected spin-orbit coupling but this can be included easily into the formalism. The corresponding Hamiltonian is

$$H_{SO} = \lambda_{SO} \sum_{i=1}^n \mathbf{l}_i \cdot \mathbf{S}_i = \lambda_{SO} \sum_{i=1}^n \left( l_i^z S_i^z + \frac{1}{2} (l_i^+ S_i^- + l_i^- S_i^+) \right).$$

where  $\mathbf{l}_i$  ( $\mathbf{S}_i$ ) are the operators of orbital (spin) angular momentum of the  $i^{th}$  electron. The spin-orbit coupling constant  $\lambda_{SO}$  can be written as [3]

$$\lambda_{SO} = \frac{\hbar^2}{2m_e^2 c^2 r_{orb}} \left. \frac{dV_{at}}{dr} \right|_{r=r_{orb}}$$

where  $m_e$  is the electron mass,  $c$  the velocity of light,  $V_{at}$  is the atomic potential acting on the electron and  $r_{orb}$  the spatial extent of the radial wave function.

The first term on the right hand side can be translated into second quantized form easily

$$H_{SO}^{\parallel} = \lambda_{SO} \sum_{m=-l}^l \frac{m}{2} \left( c_{l,m,\uparrow}^\dagger c_{l,m,\uparrow} - c_{l,m,\downarrow}^\dagger c_{l,m,\downarrow} \right). \quad (17)$$

As regards the transverse part, we note the matrix elements of the orbital angular momentum raising/lowering operator [3]:  $\langle l, m \pm 1 | l^\pm | l, m \rangle = \sqrt{(l \mp m)(l \pm m + 1)}$  whence

$$H_{SO}^\perp = \frac{\lambda_{SO}}{2} \sum_{m=-l}^{l-1} \sqrt{(l-m)(l+m+1)} \left( c_{l,m+1,\downarrow}^\dagger c_{l,m,\uparrow} + c_{l,m,\uparrow}^\dagger c_{l,m+1,\downarrow} \right). \quad (18)$$

Spin-orbit coupling can be implemented rather easily into the exact diagonalization formalism discussed above, the main difficulty again is keeping track of the Fermi sign. Due to the fact that neither  $L^z$  nor  $S^z$  are conserved anymore the corresponding reduction of the Hilbert space is no longer possible. In 3d transition-metal compounds the spin-orbit coupling constant  $\lambda_{SO}$  for the 3d shell is rather small, of order  $\lambda_{SO} \approx 0.05$  eV and can be neglected for many purposes. In the rare-earth elements spin-orbit coupling in the 4f shell is quite strong,  $\lambda_{SO} \approx 0.5$  eV, and spin-orbit coupling must be taken into account.

### 3 Effects of the environment in the crystal

So far we have considered a single ion in vacuum. Next, we discuss how the results must be modified if the ion is embedded in a solid. We will see that the small spatial extent of the 3d or 4f radial wave functions  $R_{n,l}(r)$  suppresses the effects of the environment in a solid, so that in many cases the main effect of embedding the ion into a solid is the partial splitting of the multiplets of the free ion. As in the preceding chapter we write down everything explicitly for a 3d shell but the theory is easily transferred to other shells.

In many transition-metal compounds the 3d ions are surrounded by an approximately octahedral or tetrahedral ‘cage’ of non-metal ions such as oxygen, sulphur, arsenic. These nearest neighbor ions, which will be called ‘ligands’ in the following, have a twofold effect: first, they produce a static electric field, the so-called *crystalline electric field* or CEF, and second there may be *charge transfer* that means an electron can tunnel back and forth between a ligand orbital and a 3d-orbital of the transition metal ion due to the overlap of the respective wave functions. We discuss these effects one by one.

#### 3.1 Crystalline electric field

Let us first consider the crystalline electric field, whereby we model the ligands by  $n_c$  point charges  $Z_n e$  at the positions  $\mathbf{R}_n$ . The corresponding term in the Hamiltonian for the electrons on the ion in question is (recall that the electron charge is negative)

$$\begin{aligned} -V_{CEF}(\mathbf{r}) &= -\sum_{n=1}^{n_c} \frac{Z_n}{|\mathbf{r} - \mathbf{R}_n|} = -\frac{Z_{av}}{R_{av}} \sum_{k=0}^{\infty} \sum_{m=-k}^k \gamma_{k,m} \left( \frac{r}{R_{av}} \right)^k \sqrt{\frac{4\pi}{2k+1}} Y_{k,m}(\vartheta, \varphi), \\ \gamma_{k,m} &= \sqrt{\frac{4\pi}{2k+1}} \sum_{n=1}^{n_c} \frac{Z_n}{Z_{av}} \left( \frac{R_{av}}{R_n} \right)^{k+1} Y_{k,m}^*(\vartheta_n, \varphi_n). \end{aligned} \quad (19)$$

Here we have again used multipole expansion (4) of the Coulomb potential and introduced the average distance and charge of the ligands,  $R_{av}$  and  $Z_{av}$ . Going over to  $2^{nd}$  quantization the Hamiltonian becomes [6]

$$H_{CEF} = \sum_{i,j} V_{CEF}(\nu_i, \nu_j) c_{\nu_i}^\dagger c_{\nu_j},$$

$$V_{CEF}(\nu_1, \nu_2) = \int dx \psi_{\nu_1}^*(x) V_{CEF}(\mathbf{r}) \psi_{\nu_2}(x), \quad (20)$$

where the wave functions  $\psi_\nu(x)$  are again given by (3). In calculating  $V_{CEF}(\nu_1, \nu_2)$  we start with the sum over  $\sigma$  and find a factor of  $\delta_{\sigma_1, \sigma_2}$ . The integral over the polar angles ( $\vartheta, \varphi$ ) again gives a factor of  $\delta_{m_1, m_1+m_2}$  and a Gaunt coefficient. As for the integral over  $r$  we note that the radial dependence of the wave functions  $\psi_\nu(x)$  is given by  $R_{3,2}(r)$ , which differs appreciably from zero only in a narrow range  $r \leq r_{3d}$ . Then we find

$$V_{CEF}(\nu_1, \nu_2) = \delta_{\sigma_1, \sigma_2} \sum_k \gamma_{k, m_1-m_2} c^k(2, m_1; 2, m_2) I_k,$$

$$I_k = -\frac{Z_{av} e^2}{R_{av}} \left( \frac{r_{3d}}{R_{av}} \right)^k \int_0^\infty d\rho \rho^{k+2} \tilde{R}_{nl}^2(\rho). \quad (21)$$

Here we have introduced the dimensionless variable  $\rho = r/r_{3d}$ , and the dimensionless wave function  $\tilde{R}_{nl}(\rho) = r_{3d}^{3/2} R_{nl}(\rho r_{3d})$ . Since this has a range of unity and

$$\int_0^\infty d\rho \rho^2 \tilde{R}_{nl}^2(\rho) = 1$$

we expect that the dimensionless radial integral in  $I_k$  is of order unity so that  $I_k \propto \left( \frac{r_{3d}}{R_{av}} \right)^k$ . As expected, a small  $r_{3d} \ll R_{av}$  suppresses the effect of the environment and the sum over  $k$  usually can be terminated after the lowest  $k > 0$  for which  $\gamma_{k,m}$  does not vanish for some  $m$ . Moreover, for a  $d$ -shell it again follows from the triangular condition for the Gaunt coefficients that  $k \leq 4$  and from parity that  $k$  only be even. The term with  $k = 0$  gives merely a constant shift and can be omitted so that only  $k = 2$  and  $k = 4$  need to be considered. As was the case for the Coulomb interaction, the CEF can be described by very few – in fact only one if only the lowest order in  $r_{3d}/R_{av}$  is kept – parameters  $I_k$  which depend on the radial wave function  $R_{3,2}(r)$ . These parameters again are frequently fitted to experiment. The actual form of the matrix elements then depends on the geometry of the ‘cage’ of ligands via the sums  $\gamma_{k,m}$ .

As an example let us consider the case of an ideal octahedron of identical charges. More precisely, let the nucleus of the transition-metal ion be the origin of the coordinate system, and six identical charges  $eZ$  be located at  $(\pm R, 0, 0)$ ,  $(0, \pm R, 0)$  and  $(0, 0, \pm R)$ . This means that  $R_n = R = R_{av}$  and  $Z_n = Z = Z_{av}$ , whence

$$\gamma_{k,m} = \sqrt{\frac{4\pi}{2k+1}} \sum_{n=1}^6 Y_{k,m}^*(\vartheta_n, \varphi_n). \quad (22)$$

We divide the six charges into two groups: group 1 comprises the four charges in the  $x$ - $y$  plane at  $(\pm R, 0, 0)$  and  $(0, \pm R, 0)$ . These have  $\vartheta_n = \frac{\pi}{2}$  and  $\varphi_n = \frac{n\pi}{2}$  with  $n = 0, 1, 2, 3$ . Since

$Y_{l,m}(\vartheta, \varphi) = P_{l,m}(\vartheta) e^{im\varphi}$ , we find that the contribution of group 1 to  $\gamma_{k,m}$  is proportional to

$$\sum_{n=0}^3 \left( e^{\frac{im\pi}{2}} \right)^n = \begin{cases} \frac{(e^{2\pi i})^m - 1}{e^{\frac{im\pi}{2}} - 1} = 0 & e^{\frac{im\pi}{2}} \neq 1, \\ 4 & e^{\frac{im\pi}{2}} = 1. \end{cases}$$

The four charges of group 1 therefore give a nonvanishing contribution only for  $m = 0, 4$ . Group 2 comprises the two charges at  $(0, 0, \pm R)$ . Inspection of tables of spherical harmonics [4] shows that always

$$Y_{lm}(\vartheta, \varphi) \propto \sin^m(\vartheta) e^{im\varphi} = \left( \frac{x+iy}{r} \right)^m,$$

so that the charges of group 2 contribute only for  $m = 0$ .

Combining everything we see that for the ideal octahedron we need to actually evaluate the sum (22) only for  $Y_{2,0}$ ,  $Y_{4,0}$  and  $Y_{4,\pm 4}$  whereby for the last case only the charges in the  $x$ - $y$  plane need to be considered. We start with  $Y_{2,0}$  and note that  $Y_{2,0}(\vartheta, \varphi) \propto 3 \cos^2(\vartheta) - 1$  [4]. It follows that  $\sum_{n=1}^6 Y_{2,0}(\vartheta_n, \varphi_n) \propto 4 \cdot (-1) + 2 \cdot 2 = 0$ , so that  $Y_{2,0}$  does not contribute. Using the expressions [4]

$$Y_{4,0}(\vartheta, \varphi) = \frac{3}{16} \sqrt{\frac{1}{\pi}} \cdot (35 \cos^4 \vartheta - 30 \cos^2 \vartheta + 3)$$

$$Y_{4,4}(\vartheta, \varphi) = \frac{3}{16} \sqrt{\frac{35}{2\pi}} \cdot \sin^4 \vartheta \cdot e^{4i\varphi}$$

we then find after straightforward calculation

$$\gamma_{4,0} = \sqrt{\frac{49}{4}} \quad \text{and} \quad \gamma_{4,4} = \sqrt{\frac{35}{8}}, \quad (23)$$

as well as  $\gamma_{4,-4} = \gamma_{4,4}$ . Using the tabulated values of the  $c^A(2, m; 2, m')$  (see Appendix),  $V_{CEF}(\nu_1, \nu_2)$  can be written as  $\delta_{\sigma_1, \sigma_2}$  times a matrix in the indices  $m_1$  and  $m_2$

$$V_{CEF}(m_1, m_2) = \frac{I_4}{6} \begin{pmatrix} 1 & 0 & 0 & 0 & 5 \\ 0 & -4 & 0 & 0 & 0 \\ 0 & 0 & 6 & 0 & 0 \\ 0 & 0 & 0 & -4 & 0 \\ 5 & 0 & 0 & 0 & 1 \end{pmatrix}. \quad (24)$$

This matrix has the eigenvalues  $I_4$  (twofold degenerate) with corresponding eigenfunctions

$$d_{x^2-y^2}(\Omega) = \frac{1}{\sqrt{2}} (Y_{2,-2}(\Omega) + Y_{2,2}(\Omega)) = \sqrt{\frac{15}{16\pi}} \frac{x^2-y^2}{r^2},$$

$$d_{3z^2-r^2}(\Omega) = Y_{2,0}(\Omega) = \sqrt{\frac{5}{16\pi}} \frac{3z^2-r^2}{r^2}, \quad (25)$$



and  $-2I_4/3$  (threefold degenerate) with eigenfunctions

$$\begin{aligned} d_{xy}(\Omega) &= \frac{i}{\sqrt{2}}(Y_{2,-2}(\Omega) - Y_{2,2}(\Omega)) = \sqrt{\frac{15}{4\pi}} \frac{xy}{r^2}, \\ d_{yz}(\Omega) &= \frac{i}{\sqrt{2}}(Y_{2,-1}(\Omega) + Y_{2,1}(\Omega)) = \sqrt{\frac{15}{4\pi}} \frac{yz}{r^2}, \\ d_{xz}(\Omega) &= \frac{1}{\sqrt{2}}(Y_{2,-1}(\Omega) - Y_{2,1}(\Omega)) = \sqrt{\frac{15}{4\pi}} \frac{xz}{r^2}. \end{aligned} \quad (26)$$

The two eigenfunctions for eigenvalue  $I_4$  are called  $e_g$  orbitals, whereas the three eigenfunctions for eigenvalue  $-2I_4/3$  are called  $t_{2g}$  orbitals. If the ligands are  $O^{2-}$  ions,  $Z=-2$  whence  $I_4 > 0$ , i.e., the  $e_g$  orbitals are higher in energy than the  $t_{2g}$  orbitals. This can be readily understood by comparing the  $d_{xy}$  and the  $d_{x^2-y^2}$  orbital. In the  $x$ - $y$  plane the lobes of  $d_{x^2-y^2}$  are along the axes and point directly towards the negative charges at  $(\pm R, 0, 0)$  and  $(0, \pm R, 0)$ , whereas the lobes of the  $d_{xy}$  orbital point along the diagonals and thus optimally avoid these negative charges. For the negatively charged electron, it is therefore energetically advantageous to be in the  $d_{xy}$  orbital. The splitting between the eigenvalues is frequently called  $10Dq = E(e_g) - E(t_{2g})$ , so that in our point-charge model  $Dq = I_4/6$ .

Note that the five functions  $d_\alpha(\Omega)$  in (25) and (25) are pairwise orthogonal. This means that they are obtained by a unitary transformation from the five original spherical harmonics  $Y_{2,m}(\Omega)$  and can be used as basis functions. These functions are of utmost importance in the theoretical discussion of elements with partially filled  $d$ -shells and are can be found again and again in the literature. Polar plots of these functions also can be found in the literature [4].

We see that for octahedral coordination the effect of the CEF on a  $3d$  level can be summarized in a single parameter  $10Dq$ , which may for example be obtained by a fit to experiment. This way of dealing with the CEF is very similar in spirit to our treatment of the Coulomb interaction, in that details of the radial wave functions  $R_{n,l}(r)$  are absorbed into numerical parameters which can be adjusted to experiment. Alternatively, the numerical value of  $10Dq$  for a given solid may also be obtained from a fit to a density functional band structure.

By adding  $H_{CEF}$ , which is a quadratic form in the operators  $c_\nu^\dagger/c_\nu$ , to the Hamiltonian for the intra-atomic Coulomb interaction discussed above we can now discuss the splitting of the original multiplets of the free ion under the influence of the electrostatic potential of the environment. The following should be noted: the above discussion refers to the wave function of a *single electron*. The multiplets, however, are collective eigenstates of all  $n$  electrons in an atomic shell which are created by the Coulomb interaction between electrons. The question of how these collective states split in a cubic environment is not at all easy to answer. One way would be exact diagonalization including the term  $H_{CEF}$ .

Plots of the energies of the resulting ‘crystal-field multiplets’ versus  $10Dq$  are called Tanabe-Sugano diagrams [10]. An example is shown in Figure 3.1 which shows the eigenenergies of the  $d^8$  and  $d^7$  configuration with Coulomb interaction and increasing cubic CEF,  $10Dq$ . One realizes that the highly degenerate multiplets of the free ion are split into several levels of lower degeneracy by the CEF, which is to be expected for a perturbation which lowers the symmetry.

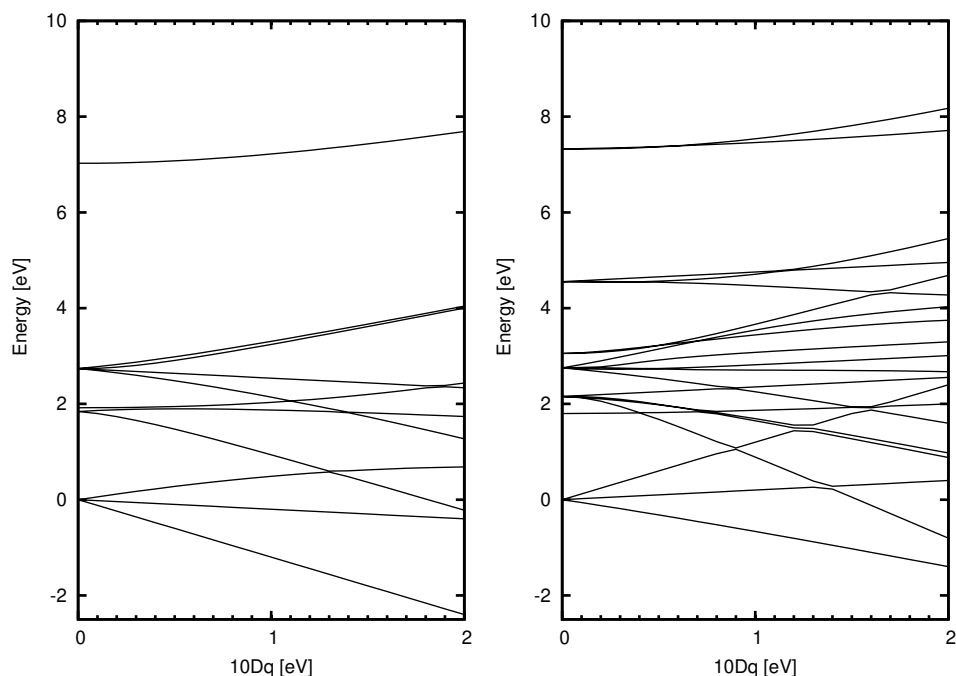


**Fig. 3:** Examples for Tanabe-Sugano diagrams: the splitting of multiplets of  $d^8$  (left) and  $d^7$  (right) for increasing  $10Dq$ . The Slater-Condon parameters have the values given in Table 2.

Note that the components into which a given multiplet splits all have the same spin as the multiplet itself. This is because the spin of an electron does not ‘feel’ an electrostatic potential; or, more precisely, because the operator of total spin commutes with any operator which acts only on the real-space coordinates  $\mathbf{r}_i$  of the electrons.

An interesting example for the application of the Tanabe-Sugano diagrams are transition-metal ions in aqueous solution. In fact, the preference of transition-metal ions for an environment with cubic symmetry is so strong that such immersed ions often surround themselves with an octahedron of water molecules. Thereby the dipole moments of these six molecules all point away from the ion and thus create an electric field which cubic symmetry which again gives rise to an  $e_g-t_{2g}$  splitting. Optical transitions between the CEF-split multiplets, which are possible only due to slight distortions of the octahedron or the generation/annihilation of vibrational quanta during the transition, correspond to frequencies in the visible range and result in the characteristic colors of such solutions. The Tanabe-Sugano diagrams have proved to be a powerful tool to understand the absorption spectra of such solutions [8]. By matching the energies of the observed transitions to energy differences in the Tanabe-Sugano diagrams one can extract estimates for the Slater-Condon parameters and for  $10Dq$ . The values of the Slater-Condon parameters turn out to be somewhat smaller than those for ions in vacuum due to dielectric screening in the solution. An independent estimate for  $10Dq$  can also be extracted from measured heats of hydration – this is because both  $10Dq$  and the electrostatic energy of the system ‘ion plus octahedron’ depend on the distance between the transition-metal ion and the water molecules – and compared to the estimate from the absorption spectrum whereby good agreement is usually obtained [11].

### 3.2 Charge transfer

We continue our discussion of a transition-metal ion at the origin of the coordinate system surrounded by a ‘cage’ of  $n$  ligands at  $\mathbf{R}_n$ . The second mechanism by which the ligands may influence the energy levels of the transition metal ion is *charge transfer*. This means that the  $3d$  levels of the transition metal ion hybridize with atomic orbitals on the ligands which shifts the energies of the  $3d$  levels. To understand how this happens, let us consider a toy Hamiltonian which describes just a single ‘ $d$ -orbital’  $|\psi_1\rangle$  with energy  $\varepsilon_1$  coupled to a single ‘ligand orbital’  $|\psi_2\rangle$  with energy  $\varepsilon_2$

$$H = \sum_{i=1}^2 \varepsilon_i c_i^\dagger c_i - (t c_1^\dagger c_2 + H.c.)$$

We have suppressed the spin index and the meaning of the creation/annihilation operators should be self-evident). The hybridization matrix element  $-t = \langle \psi_1 | H | \psi_2 \rangle$  thereby originates from the overlap of the atomic wave functions and facilitates the transfer of an electron between the two orbitals. The ansatz  $|\psi\rangle = u|\psi_1\rangle + v|\psi_2\rangle$  for an eigenstate readily leads to the  $2 \times 2$  matrix

$$h = \begin{pmatrix} \varepsilon_1 & -t \\ -t & \varepsilon_2 \end{pmatrix}, \quad (27)$$

whose eigenvalues are

$$E_{\pm} = \frac{\varepsilon_1 + \varepsilon_2}{2} \pm \sqrt{\left(\frac{\varepsilon_1 - \varepsilon_2}{2}\right)^2 + t^2}.$$

We may assume without loss of generality that  $\varepsilon_1 > \varepsilon_2$ , whence  $\sqrt{\left(\frac{\varepsilon_1 - \varepsilon_2}{2}\right)^2 + t^2} = \frac{\varepsilon_1 - \varepsilon_2}{2} + \Delta$ , with some  $\Delta > 0$ . It follows that  $E_- = \varepsilon_2 - \Delta < \varepsilon_2$  and  $E_+ = \varepsilon_1 + \Delta > \varepsilon_1$ . This means that the lower level is shifted downwards by  $\Delta$ , whereas the upper level is shifted upwards by the same amount, an effect known as *level repulsion*. This mechanism can split the degeneracy of the  $3d$ -level because, depending on the geometry of the cage, different  $3d$  orbitals can have different hybridization matrix elements with the ligand orbitals.

Note that the eigenstates now are a mixture of the two orbitals. For  $t \ll \varepsilon_1 - \varepsilon_2$ , however, the weight of  $|\psi_2\rangle$  in the eigenstate for  $E_-$  is  $\left(\frac{t}{\varepsilon_1 - \varepsilon_2}\right)^2$  which means the state still has predominant  $|\psi_1\rangle$  character.

To describe charge transfer quantitatively we need to enlarge our set of Fermion operators  $c_\nu^\dagger/c_\nu$  by operators  $l_\mu^\dagger/l_\mu$  which create/annihilate electrons in orbitals centered on the ligands. We simplify matters by assuming that only  $2p$  orbitals are relevant for the ligands, as would be the case for oxygen ligands. For the rest of this paragraph on charge transfer we switch to a new set of basis functions which is more suitable for the discussion of hybridization. First, we use  $3d$  wave functions whose angular part is given by the real-valued spherical harmonics (25) and (26)

$$\psi_{\nu_i}(x) = R_{3,2}(r) d_\alpha(\Omega) \delta_{\sigma,\sigma_i}, \quad (28)$$

with  $\alpha \in \{xy, xz, yz, x^2 - y^2, 3z^2 - r^2\}$ , so that now  $\nu_i = (\alpha, \sigma)$ .

For the ligand orbitals we use wave functions whose angular part is given by the real-valued  $p$ -like spherical harmonics

$$p_x(\Omega) = \frac{1}{\sqrt{2}}(-Y_{1,1}(\Omega) + Y_{1,-1}(\Omega)) = \sqrt{\frac{3}{4\pi}} \frac{x}{r}, \quad (29)$$

$$p_y(\Omega) = \frac{i}{\sqrt{2}}(Y_{1,1}(\Omega) + Y_{1,-1}(\Omega)) = \sqrt{\frac{3}{4\pi}} \frac{y}{r}, \quad (30)$$

$$p_z(\Omega) = Y_{1,0}(\Omega) = \sqrt{\frac{3}{4\pi}} \frac{z}{r}, \quad (31)$$

and are centered on the ligands

$$\psi_{\mu_j}(x) = R_{2,1}(r_{n_j}) p_{\beta_j}(\Omega_n) \delta_{\sigma,\sigma_j}. \quad (32)$$

Here,  $\mathbf{r}_n = \mathbf{r} - \mathbf{R}_n$  and  $\beta \in \{x, y, z\}$  so that  $\mu_j = (n_j, \beta_j, \sigma_j)$ . The obvious generalization of the toy Hamiltonian then is

$$H_{CT} = \sum_i \varepsilon_{\nu_i} c_{\nu_i}^\dagger c_{\nu_i} + \sum_j \varepsilon_{\mu_j} l_{\mu_j}^\dagger l_{\mu_j} - \sum_{i,j} \left( t_{\nu_i, \mu_j} c_{\nu_i}^\dagger l_{\mu_j} + H.c. \right). \quad (33)$$

This would still not be very useful because it contains a large number of parameters, in particular the *hybridization integrals*  $-t_{\nu_i, \mu_j}$ . The crucial simplification comes about because these hybridization integrals can be expressed in terms of very few parameters by using the celebrated *Slater-Koster tables* [12]. For example, for the present case where only the  $p$  orbitals of the ligands are taken into account there are just two relevant parameters:  $V_{pd\sigma}$  and  $V_{pd\pi}$ . More precisely, a typical entry in the Slater-Koster tables looks like

$$-t_{1x, 2xy} = \sqrt{3} l^2 m V_{pd\sigma} + m (1 - 2l^2) V_{pd\pi}.$$

This gives the hopping integral  $-t_{1x, 2xy}$  between a  $p_x$  orbital on atom 1 and a  $d_{xy}$  orbital on atom 2 as a function of the components of the unit vector  $(l, m, n)$  pointing from atom 1 to atom 2. Thereby the parameters  $V_{pd\sigma}$  and  $V_{pd\pi}$  depend only on the distance between the two atoms. It is obvious from this that the hopping orbitals  $-t_{\nu_i, \mu_j}$  in Eq. (33) depend on the geometry of the ‘cage’ of ligands. By inserting the unitary transformation (25) and (26) as well as (31),  $H_{CT}$  now could be transformed to the original complex spherical harmonics  $Y_{2,m}(\Omega)$  and then be easily included into exact diagonalization formalism discussed above. The main problem is that the number of orbitals in the cluster and hence the dimension of the Hilbert space increases considerably so that one has to resort to numerical methods such as the Lanczos algorithm [13]. To illustrate the procedure and thereby show how to alleviate the problem of the increase of the Hilbert space dimension, we specialize again to the case where the ligands form an ideal octahedron, with the transition metal ion in the center of gravity. In other words, the ligands again are located at  $(\pm R, 0, 0)$ ,  $(0, \pm R, 0)$  and  $(0, 0, \pm R)$ . We want to solve the Hamiltonian (33) for this cluster of seven ions assuming that the parameters  $V_{pd\sigma}$ ,  $V_{pd\pi}$ ,  $\varepsilon_{\nu_i}$  and  $\varepsilon_{\mu_j}$  are given. For simplicity we set the energies  $\varepsilon_{\nu_i}$  of the  $3d$  orbitals equal to zero and assume that  $\varepsilon_{\mu_j} = \varepsilon > 0$

for all ligand orbitals.  $V_{pd\sigma}$  and  $V_{pd\pi}$  depend only on the distance between ligand and transition-metal ion and therefore are the same for all six ligands. Since we are retaining three  $p$ -orbitals on each ligand and the five  $d$ -orbitals on the transition-metal ion, the total number of orbitals in the cluster would be  $5 + 6 \cdot 3 = 23$ . What we would have to do is to go through all six ligands, determine  $(l, m, n)$  for each of them, set up the hopping integral between each of the five  $3d$  orbitals and each of the three  $2p$  orbitals on the respective ligand using the Slater-Koster tables. This would give us a  $23 \times 23$  matrix instead of the  $2 \times 2$  matrix (27), the eigenvalues of which would tell us how the  $3d$  orbitals are shifted by the hybridization. Fortunately enough, the high symmetry of the octahedral cluster allows us to bring the Hamiltonian to block-diagonal form and obtain analytical expressions for the energies. The key simplification comes about by constructing *hybridizing combinations* of  $2p$  orbitals on the six ligands. Consider the  $d_{xy}$  orbital in Figure 4. Using symmetry arguments or the Slater-Koster tables one can show that out of the 18  $p$  orbitals on the ligands only the four  $p$ -orbitals shown in the Figure have a nonvanishing hybridization integral with the  $d_{xy}$  orbital. These four orbitals moreover hybridize with no other  $d$  orbital. Then, we form the following linear combinations of these four orbitals:

$$\begin{aligned} |1\rangle &= \frac{1}{2} \left( \psi_{1,y}(x) + \psi_{2,x}(x) - \psi_{3,y}(x) - \psi_{4,x}(x) \right), \\ |2\rangle &= \frac{1}{2} \left( \psi_{1,y}(x) + \psi_{2,x}(x) + \psi_{3,y}(x) + \psi_{4,x}(x) \right), \\ |3\rangle &= \frac{1}{2} \left( \psi_{1,y}(x) - \psi_{2,x}(x) - \psi_{3,y}(x) + \psi_{4,x}(x) \right), \\ |4\rangle &= \frac{1}{2} \left( \psi_{1,y}(x) - \psi_{2,x}(x) + \psi_{3,y}(x) - \psi_{4,x}(x) \right), \end{aligned}$$

where we have dropped the spin index of the  $\psi_{\mu_j}(x)$  for brevity. If  $p$  orbitals on different ligands are orthogonal to each other,  $\langle \psi_{i,\alpha} | \psi_{j,\beta} \rangle = \delta_{i,j} \delta_{\alpha,\beta}$ , these four combinations are orthonormal, that means we can use them as new basis functions. Next, using the matrix elements of  $H$  indicated in Figure 4, which can be easily verified using the Slater-Koster tables, we see that

$$\langle d_{xy} | H_{CT} | i \rangle = -2V_{pd\pi} \delta_{i,1}.$$

This means that the states  $|2\rangle$ ,  $|3\rangle$  and  $|4\rangle$  do not mix with  $d_{xy}$  and since they also do not mix with any other of the five  $d$ -orbitals, they are eigenstates of  $H_{CT}$  with energy  $\varepsilon$  by construction. We thus need to keep only  $|d_{xy}\rangle$  and  $|1\rangle$  and thus arrive at exactly the same  $2 \times 2$  matrix Eq. (27) as for the toy model

$$h = \begin{pmatrix} 0 & -2V_{pd\pi} \\ -2V_{pd\pi} & \varepsilon \end{pmatrix}. \quad (34)$$

with eigenvalues  $E_{\pm} = \frac{\varepsilon}{2} \pm \sqrt{\left(\frac{\varepsilon}{2}\right)^2 + 4V_{pd\pi}^2}$ . To simplify our expressions we assume weak hybridization,  $V_{pd\pi} \ll \varepsilon$ , whence the energy of the lower eigenstate, which for  $\varepsilon > 0$  has predominantly  $|d_{xy}\rangle$  character, becomes

$$E(t_{2g}) \approx -\frac{4V_{pd\pi}^2}{\varepsilon}.$$

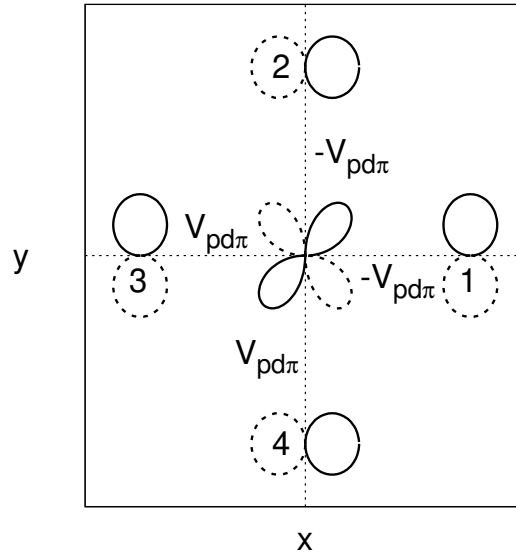


**Fig. 4:**  $p$  orbitals on ligands with nonvanishing hybridization with the  $d_{xy}$  orbital in the center. The figure shows the  $x$ - $y$  plane, lobes with positive (negative) sign are drawn by full (dashed) lines. The labels of the ligands are given next to the  $p$  orbitals, the hybridization integrals obtained from the Slater-Koster tables are indicated for each bond.

The upper eigenstate, which predominantly has ligand- $p$  character, has energy  $\varepsilon + 4V_{pd\pi}^2/\varepsilon$ . We could have proceeded in exactly the same way if instead of the  $x$ - $y$  plane we would have considered the  $x$ - $z$  or  $y$ - $z$  plane and the  $d_{xz}$  or  $d_{yz}$  orbitals. Therefore, all of the three  $t_{2g}$  orbitals are shifted by the same energy and remain degenerate in the presence of hybridization!

In a similar but slightly more complicated way one finds that the  $e_g$ -orbitals  $d_{x^2-y^2}$  and  $d_{3z^2-r^2}$  also remain degenerate and are shifted to

$$E(e_g) \approx -\frac{4V_{pd\sigma}^2}{\varepsilon}.$$

We have thus found the energy levels of the Hamiltonian (33) for the octahedral cluster with only  $p$  orbitals on the ligands: there are five states with predominant  $3d$  character and energies  $-4V_{pd\pi}^2/\varepsilon$  ( $t_{2g}$ , 3-fold degenerate) or  $-4V_{pd\sigma}^2/\varepsilon$  ( $e_g$ , 2-fold degenerate). We also have five corresponding states with predominant  $p$ -character and energies  $\varepsilon + 4V_{pd\pi}^2/\varepsilon$  (3-fold degenerate) or  $\varepsilon + 4V_{pd\sigma}^2/\varepsilon$  (2-fold degenerate). And finally we have the non-bonding combinations which have pure  $p$  character and retain their energy of  $\varepsilon$ . Obviously there must be 13 of these.

We see that charge transfer results in the same splitting into  $t_{2g}$  and  $e_g$  orbitals as the electrostatic potential due to the charges on the ligands. (In fact, it follows from the theory of irreducible representations of symmetry groups [3, 8, 10, 11] that this holds true for *any* perturbation with cubic symmetry). Therefore, if we are only interested in the energies of the eigenstates we may as well drop the ligand orbitals from the Hamiltonian and describe the splitting due to charge transfer by an ‘effective  $10Dq$ ’ given by

$$10Dq_{CT} = \frac{4}{\varepsilon}(V_{pd\pi}^2 - V_{pd\sigma}^2).$$

This would have to be added to the ‘electrostatic  $10Dq$ ’ discussed earlier.

To conclude this section, we mention that using the octahedron-shaped cluster discussed in the preceding section by the exact diagonalization method has been an extraordinarily successful method for the simulation of valence band photoemission spectra, X-ray absorption spectra, and core-level photoemission spectra of  $3d$  transition-metal compounds [14–20]. In many cases, the spectra calculated in a mere octahedron can be compared peak-by-peak to experimental spectra. This also provides unambiguous evidence that the multiplets of the free ion, slightly modified by CEF and charge transfer, do persist in the solid.

## 4 Multiband Hubbard models

We have now discussed all necessary parts of the Hamiltonian to describe transition-metal and rare-earth compounds, i.e., multiband Hubbard models. We view the solid as an array of ions with a certain number of atomic orbitals on each of them and assume that these orbitals are labeled by some index  $i$ . The position of the ion on which orbital  $i$  is centered is  $\mathbf{R}_i$ . Then, we split the orbitals in the solid into two groups: the correlated and the uncorrelated orbitals. The correlated orbitals have radial wave functions with small spatial extent and the Coulomb interaction between electrons in these orbitals is strong. The uncorrelated orbitals are more extended and the Coulomb interaction between electrons in these orbitals is weak enough to be neglected. Of course, this division of the orbitals is arbitrary to some extent. In principle, one might also include Coulomb interaction between electrons in orbitals on different ions but we neglect this because it will in general be much weaker than the interaction between electrons on the same ion.

Then, the problem arises how to choose these orbitals. For example for a  $d$  shell we could choose orbitals whose radial part is given by the spherical harmonics  $Y_{2,m}(\Omega)$  but we might as well choose the real-valued spherical harmonics  $d_\alpha(\Omega)$  in (25) and (26). The preceding discussion has shown that the  $Y_{l,m}(\Omega)$  are convenient for the discussion of ‘purely atomic’ aspects of the problem, such as the Coulomb interaction within atomic shells and the spin-orbit coupling, whereas the real-valued spherical harmonics  $d_\alpha(\Omega)$  are more convenient for ‘solid related’ aspects such as inter-ion hopping and CEF splitting. Since the  $Y_{l,m}(\Omega)$  and the  $d_\alpha(\Omega)$  are related by a unitary transformation this is more of a notational problem. Next, we introduce creation/annihilation operators  $c_{\nu_i}^\dagger/c_{\nu_i}$  for electrons in these orbitals. Thereby we choose the compound index  $\nu_i = (\mathbf{R}_i, n_i, l_i, m_i, \sigma_i)$  for Coulomb interaction and spin-orbit coupling and  $\nu_i = (\mathbf{R}_i, n_i, l_i, \alpha_i, \sigma_i)$  with  $\alpha_i \in \{s, p_x, p_y, p_z, d_{xy}, \dots\}$  for the inter-ion hopping and CEF. The inter-ion hopping is obtained by generalizing (33)

$$H_0 = \sum_i \varepsilon_{\nu_i} c_{\nu_i}^\dagger c_{\nu_i} - \sum_{i \neq j} \left( t_{\nu_i, \nu_j} c_{\nu_i}^\dagger c_{\nu_j} + H.c. \right). \quad (35)$$

The hopping integrals  $-t_{\nu_i, \nu_j}$  again can be expressed in terms of relatively few  $V$ -parameters via the Slater-Koster tables, the numerical values of the  $V$ -parameters and the energies  $\varepsilon_{\nu_i}$  can be obtained by fit to a density functional band structure. For the correlated orbitals thereby extra care is necessary due to the ‘double counting problem’ (see, e.g., Ref. [21]).

Moreover, we add for each ion the electrostatic part of the CEF, (20). So far the Hamiltonian is a quadratic form in Fermion operators and can always be solved after Fourier transform.

Next, for the correlated orbitals we add the Coulomb interaction (2) with the matrix elements (9). Since we are considering only the Coulomb interaction within a given atomic shell, all four  $c_{\nu_i}^\dagger/c_{\nu_i}$  operators in each term of (2) must have the same  $\mathbf{R}_i$ . The Hamiltonian now is quartic in Fermion operators and thus not solvable anymore. Rather, we have to resort to one of the many approximation schemes known so far for correlated electrons. Finally we may also add the spin-orbit coupling. Whether this is necessary depends on the magnitude of the spin-orbit coupling constant  $\lambda_{SO}$ . Since spin-orbit coupling is a relativistic effect,  $\lambda_{SO}$  is larger for heavy elements. It is more or less negligible for  $3d$  ions, but important for  $5d$  transition metals or  $4f$  rare earths.

It is obvious that the resulting Hamiltonian is quite complicated and it is highly desirable to simplify it. There are several possible ways to do so.

1. ‘Integrating out’ uncorrelated orbitals which act only to connect correlated orbitals.

To see what this means, consider the toy Hamiltonian for three orbitals  $|d_1\rangle$ ,  $|d_2\rangle$  and  $|l\rangle$ :

$$H = \Delta l^\dagger l - t \left( d_1^\dagger l + l^\dagger d_1 + d_2^\dagger l + l^\dagger d_2 \right),$$

where we have dropped the spin index for simplicity and the meaning of the Fermion operators should be obvious. It may be viewed as describing a ‘bond’ connecting the two ‘ $d$ -orbitals’  $|d_1\rangle$  and  $|d_2\rangle$  (which have an energy of zero) via the ‘bridging orbital’  $|l\rangle$  which has energy  $\Delta$ . We introduce the bonding/antibonding combinations  $d_\pm^\dagger = \frac{1}{\sqrt{2}} (d_1^\dagger \pm d_2^\dagger)$  whence the Hamiltonian becomes

$$H = \Delta l^\dagger l - \sqrt{2}t \left( d_+^\dagger l + l^\dagger d_+ \right).$$

the *ansatz*  $|\psi\rangle = (A_+ d_+^\dagger + A_l l^\dagger + A_- d_-^\dagger)|0\rangle$  then leads to the  $3 \times 3$  Hamilton matrix

$$h = \begin{pmatrix} 0 & -\sqrt{2}t & 0 \\ -\sqrt{2}t & \Delta & 0 \\ 0 & 0 & 0 \end{pmatrix},$$

which has eigenvalues  $E = 0, (\Delta \pm \sqrt{\Delta^2 + 8t^2})/2$ . For the sake of simplicity we consider the limit  $\Delta \gg t$  whence the energies become  $E = 0, \Delta + 2t^2/\Delta, -t^2/\Delta$ . The eigenfunction for  $E_1 = 0$  is  $|\psi_1\rangle = d_-^\dagger|0\rangle$ , the one for  $E_2 = -2t^2/\Delta$  is  $|\psi_2\rangle \approx d_+^\dagger|0\rangle$  and the one for  $E_3 = \Delta + 2t^2/\Delta$  is  $|\psi_3\rangle \approx l^\dagger|0\rangle$ . In other words, the wave function for the high energy state  $E_3$  has mainly ‘bridging orbital’ character, whereas those of the two low energy states  $E_1$  and  $E_2$  have predominant  $d$ -character. Now consider the effective Hamiltonian

$$H_{eff} = -\frac{t^2}{\Delta} \sum_{i=1,2} d_i^\dagger d_i - \frac{t^2}{\Delta} \left( d_1^\dagger d_2 + H.c. \right).$$

It is obvious that the eigenenergies and corresponding eigenstates of  $H_{eff}$  are the same as the two low energy eigenstates of the original Hamiltonian. In other words,  $H_{eff}$  describes



the *low energy sector* of the full Hamiltonian and the high-energy bridging orbital has disappeared.

With this reasoning, one is often omitting uncorrelated ‘bridging orbitals’ from the Hamiltonian  $H_0$  and uses an effective  $\tilde{H}_0$  that comprises only the correlated orbitals and ‘effective hopping integrals’. The latter can again be obtained by a fit to the band structure, whereby however only bands with predominant *d*-character must be taken into account. Clearly, this reduces the number of orbitals which is important if one uses numerical methods.

2. Taking the limit of large CEF or, in the simplest case where the correlated electrons are in octahedral coordination, the limit of large  $10Dq$ . Then, one may restrict the basis to states where the numbers of electrons in the  $t_{2g}$  and  $e_g$  orbitals are fixed. For example, for  $\text{Ni}^{2+}$  (i.e.  $d^8$ ) in cubic symmetry one may assume in the limit of large  $10Dq$  that the six  $t_{2g}$ -orbitals always are completely filled. Then, one needs to consider only the two electrons in the partially filled  $e_g$  level, resulting in a significant reduction of the number of possible basis states. Similarly, for compounds containing early transition metals such as Scandium, Titanium or Vanadium, one often assumes that the  $e_g$  orbitals are so high in energy that only the  $t_{2g}$  orbitals need to be taken into account.
3. Finally, one may use the simplified form of the Coulomb interaction as in Eq. (14).

An example for this ‘reduction process’ can be found in the paper by Craco *et al.* [22] where the authors discuss the photoemission and inverse photoemission spectrum of  $\text{SmO}_{1-x}\text{F}_x\text{FeAs}$  thereby using a Hamiltonian which contains only the five Fe  $3d$  orbitals and a Coulomb interaction of precisely the form (14) where  $U_{m,m'}$  and  $J_{m,m'}$  are replaced by average values.

## 5 Conclusion

We have seen that the Coulomb repulsion between electrons in partially filled atomic shells leads to multiplet splitting. The multiplets may be viewed as collective excitations of the ‘not-so-many-body-system’ formed by the electrons in the shell. We have seen that a relatively simple theory—essentially degenerate first order perturbation theory—describes the energies of the multiplets quite well and gives a good description of the line spectra of free atoms. If transition metal atoms are embedded into a solid the collective excitations of the electrons in their partly filled  $3d$  shells are modified by the crystalline electric field of their environment and by hybridization with orbitals on neighboring atoms. If these effects are taken into account, which is relatively easy if one uses the exact diagonalization method, the resulting ‘extended multiplet theory’ turns out to be quite successful in reproducing a wide variety of experimental results for transition metal compounds. While this ‘extended multiplet theory’ refers to a single transition metal ion, we have also seen that there are simplifications and extensions of this theory to lattice systems, i.e., the multiband Hubbard models. These then are the appropriate models to describe compounds containing  $3d$  or  $4d$  transition metal ions.

### A Gaunt coefficients

$m$	$m'$	$c^0$	$7 c^2$	$21 c^4$	$a^0$	$49 a^2$	$441 a^4$	$b^0$	$49 b^2$	$441 b^4$
$\pm 2$	$\pm 2$	1	-2	1	1	4	1	1	4	1
$\pm 2$	$\pm 1$	0	$\sqrt{6}$	$-\sqrt{5}$	1	-2	-4	0	6	5
$\pm 2$	0	0	-2	$\sqrt{15}$	1	-4	6	0	4	15
$\pm 1$	$\pm 1$	1	1	-4	1	1	16	1	1	16
$\pm 1$	0	0	1	$\sqrt{30}$	1	2	-24	0	1	30
0	0	1	2	6	1	4	26	1	4	36
$\pm 2$	$\mp 2$	0	0	$\sqrt{70}$	1	4	1	0	0	70
$\pm 2$	$\mp 1$	0	0	$-\sqrt{35}$	1	-2	-4	0	0	35
$\pm 1$	$\mp 1$	0	$-\sqrt{6}$	$-\sqrt{40}$	1	1	16	0	6	40

**Table 5:** Gaunt coefficients  $c^k(2, m; 2, m')$ , and the  $a^k(2, m; 2, m')$  and  $b^k(2, m; 2, m')$

$m$	$m'$	$c^0$	$15 c^2$	$33 c^4$	$\frac{429}{5} c^6$
$\pm 3$	$\pm 3$	1	-5	3	-1
$\pm 3$	$\pm 2$	0	5	$-\sqrt{30}$	$\sqrt{7}$
$\pm 3$	$\pm 1$	0	$\sqrt{10}$	$\sqrt{54}$	$-\sqrt{28}$
$\pm 3$	0	0	0	$-\sqrt{63}$	$\sqrt{84}$
$\pm 2$	$\pm 2$	1	0	-7	6
$\pm 2$	$\pm 1$	0	$\sqrt{15}$	$\sqrt{32}$	$-\sqrt{105}$
$\pm 2$	0	0	$-\sqrt{20}$	$-\sqrt{3}$	$4\sqrt{14}$
$\pm 1$	$\pm 1$	1	3	1	-15
$\pm 1$	0	0	$\sqrt{2}$	$\sqrt{15}$	$5\sqrt{14}$
0	0	1	4	6	20
$\pm 3$	$\mp 3$	0	0	0	$-\sqrt{924}$
$\pm 3$	$\mp 2$	0	0	0	$\sqrt{462}$
$\pm 3$	$\mp 1$	0	0	$\sqrt{42}$	$-\sqrt{210}$
$\pm 2$	$\mp 2$	0	0	$\sqrt{70}$	$\sqrt{504}$
$\pm 2$	$\mp 1$	0	0	$-\sqrt{14}$	$-\sqrt{378}$
$\pm 1$	$\mp 1$	0	$-\sqrt{24}$	$-\sqrt{40}$	$-\sqrt{420}$

**Table 6:** The Gaunt coefficients  $c^k(3, m; 3, m')$

## References

- [1] J.H. de Boer and E.J.W. Verwey, Proc. Phys. Soc. London 49, 59 (1937)
- [2] Yu. Ralchenko, A.E. Kramida, J. Reader, and NIST ASD Team  
NIST Atomic Spectra Database (ver. 4.1.0), (2011)  
<https://physics.nist.gov/asd>
- [3] L.D. Landau and E.M. Lifshitz: *Course of Theoretical Physics*  
(Pergamon Press, Oxford New York, 1977)
- [4] *Table of spherical harmonics* (Wikipedia)  
[https://en.wikipedia.org/wiki/Table\\_of\\_spherical\\_harmonics](https://en.wikipedia.org/wiki/Table_of_spherical_harmonics)
- [5] J.D. Jackson: *Classical Electrodynamics* (Wiley, New York, 1999)
- [6] A.L. Fetter and J.D. Walecka: *Quantum Theory of Many Particle Systems*  
(McGraw-Hill, San Francisco, 1971)
- [7] J.C. Slater: *Quantum Theory of Atomic Structure*  
(McGraw-Hill, New York, 1960)
- [8] J.S. Griffith: *The Theory of Transition Metal Ions*  
(Cambridge University Press, Cambridge, 1961)
- [9] M. Haverkort, PhD Thesis (Universität zu Köln, 2005)
- [10] S. Sugano, Y. Tanabe, and H. Kitamura: *Multiplets of Transition Metal Ions*  
(Academic Press, New York 1970)
- [11] B.N. Figgis: *Introduction to Ligand Fields*  
(Interscience Publishers, New York London Sydney, 1966)
- [12] J.C. Slater and G.F. Koster, Phys. Rev. **94**, 1498 (1954)  
For an online version of the tables see *Tight binding* (Wikipedia)  
[https://en.wikipedia.org/wiki/Tight\\_binding](https://en.wikipedia.org/wiki/Tight_binding)
- [13] E. Koch: *The Lanczos Method* in E. Pavarini, E. Koch, and P. Coleman (eds.):  
*Many-Body Physics: From Kondo to Hubbard*  
Modeling and Simulation, Vol. 5 (Forschungszentrum Jülich, 2015)
- [14] A. Fujimori and F. Minami, Phys. Rev. B **30**, 957 (1984)
- [15] J. van Elp, J.L. Wieland, H. Eskes, P. Kuiper, G.A. Sawatzky, F.M.F. de Groot, and  
T.S. Turner, Phys. Rev. B **44**, 6090 (1991)
- [16] A. Fujimori, N. Kimizuka, T. Akahane, T. Chiba, S. Kimura, F. Minami,  
K. Siratori, M. Taniguchi, S. Ogawa, and S. Suga, Phys. Rev. B **42**, 7580 (1990)

- 
- [17] F.M.F. de Groot, *Journal of Electron Spectroscopy and Related Phenomena*, **67** 525 (1994)
- [18] M. Finazzi, N.B. Brookes, and F.M.F. de Groot, *Phys. Rev. B* **59**, 9933 (1999)
- [19] F.M.F. de Groot, *Coordination Chemistry Reviews*, **249** 31 (2005)
- [20] F.M.F. de Groot and A. Kotani: *Core Level Spectroscopy of Solids*  
(Taylor & Francis, Abingdon on Thames, 2008)
- [21] I.A. Nekrasov, N.S. Pavlov, and M.V. Sadovskii, *JETP Lett.* **95**, 581 (2012)
- [22] L. Craco, M.S. Laad, S. Leoni, and H. Rosner, *Phys. Rev. B* **78**, 134511 (2008)